Synthesis of some Hydrazone derivatives via MgO nanoparticle as a promising and efficient heterogeneous catalyst under solvent-free and ultrasonic conditions

Hossein Moradi
University of Kashan
Mohsen Moradian (m.moradian@kashanu.ac.ir)
University of Kashan

Research Article

Keywords: MgO nanoparticles, hydrazones, condensation, nanocatalyst, ultrasonic reaction

Posted Date: July 20th, 2023

DOI: https://doi.org/10.21203/rs.3.rs-3175791/v1

Abstract

A green protocol with high productivity for synthesizing hydrazone derivatives through condensation method between aromatic hydrazines and aldehydes and ketones is described. In this procedure, we used magnesium oxide nanoparticles as a green catalyst to access hydrazones under solvent-free and ultrasonic conditions. The present strategy provided essential improvements for the synthesis of hydrazones including clean reaction, non-acidic and solvent-free conditions. The MgO nanoparticle has acid-base bifunctional sites, which make it an appropriate candidate for the preparation of synthetically valuable hydrazone derivatives, and all desired compounds were synthesized with high yields under mild conditions.

1. INTRODUCTION

Hydrazones are of profound importance due to their wide applications in organic synthesis, chemical industry, and biological systems [1]. Hydrazones represented a broad range of remarkable biological activities, including anti-HIV, antimalarial, anti-inflammatory, antitumor, and antibiotic properties (Fig. 1) [2]. They also can act as a drug carrier for site-specific delivery, particularly for anticancer and antibacterial agents [3]. Moreover, this class of compounds are employed as a new strategy for direct functionalization of hydrazones derived from aldehyde through radical addition to the C = N bond in hydrazone [4]. Furthermore, hydrazones can be employes as ligands of metal complexes and covalent organic frameworks [5], dyes [6], hole-transporting materials [7], and therapeutic agents [8]. In addition, they have been extensively investigated in the context of supramolecular chemistry owing to their unique structural properties, which enable them to apply as molecular switches, Metallo-assemblies, and sensors [9]. The reversibility of hydrazone's bond formation is a useful feature in dynamic combinatorial chemistry [10]. Among these interesting properties, they also are categorized as an important intermediate in synthetic organic chemistry, including Fischer synthesis [11].

Given such significance, hydrazones received the high attention of the synthetic community in recent years [12]. Many synthetic routes have demonstrated to achieve hydrazone compounds. Meanwhile, the most straightforward route to synthesize hydrazone bond compounds is the coupling between hydrazines and carbonyl group in aldehydes and ketones [9]. The readily obtained compounds usually need a simple purification process due to the highly crystalline features of the product that crash out of the reaction mixture. Some of the recently reported methods also include catalytic procedures suffering from limitations, including excessive use of starting materials and solvents like Methanol. So, introducing milder conditions to access hydrazones is highly demanded [13].

In recent decades, researchers have been interested in developing and designing new routes and materials with eco-friendly properties [14]. To achieve this goal, nanoscience could be the solution. A significant aspect of nanoscience is its ability to develop new routes for synthesizing various nanoparticles (NPs) with different chemical compositions, sizes, shapes, and properties. Nanocatalysis is a rapidly growing field that provides new nanomaterials with wide application, including homogeneous

and heterogeneous catalytic systems. Meanwhile, magnesium oxide (MgO) NPs are known as an important class of nanomaterials with great applications in organic synthesis which could be used as both individual catalysts and catalysts support in various transformations [14].

Herein, we wish to report an efficient and convenient method for condensation of aryl hydrazines and various aromatic aldehydes and ketones to get corresponding hydrazone derivatives. In this report, we use magnesium oxide nanoparticles as a green catalyst to promote this transformation under solvent-free and ultrasonic conditions.

2. MATERIALS AND METHOD

All applied chemicals and reagents in this report, were commercially available and purchased from various companies such as Merck and Sigma-Aldrich. All the materials were applied without further purifications. The standard procedures were performed to purify solvents before using them in the reaction.

The analysis of scanning electron microscope (SEM) for the nanoparticle was performed on a FESEM Hitachi S4160. The recorded IR spectra was achieved on a Nicolet FT-IR spectrophotometer and the samples were prepared as KBr pellets. To record 1H and 13C NMR spectra, d6-DMSO was used as the proper solvent. The mentioned spectra were recorded on a Bruker DRX-400 spectrometer. X'PertPro (Philips) instrument was used to record XRD patterns applying 1.54 A° wavelengths of the X-ray beam which belongs to Cu anode material. Transmission electron microscopy (TEM) was achieved on a Jeol JEM-2100UHR apparatus. The analysis was operated at 200 kV. Finally, melting points were measured with a Yanagimoto micro melting point device. The reported data were recorded without further correction. The reaction monitoring and clarifying purity of the substrates were performed by TLC on silica-gel polygram SILG/UV 254 plates (from Merck Company).

3. EXPERIMENTAL

3.1. Catalyst preparation

In order to synthesize MgO nanoparticles, the reported procedure by Chan et al. [15] have been used with modifications. In this method, the sol-gel process has been performed to achieve MgO nanoparticles. 14.2 g of magnesium acetate and 9 g of oxalic acid as gelation agent was dissolved in 20 mL Ethanol separately. Then, the prepared solutions has been mixed, and the gel-magnesium resin has been achieved at PH 5. This solution stirred for 12 h at ambient temperature. Then, to obtain the sol-gel powder, the produced resin was dried by stirring the solution for 24 h at 100°C. The ultimate product was calcined at 500°C temperatures in air for 2 h to obtain the white powder of MgO.

3.2. The procedures for the synthesis of hydrazone derivatives by MgO nanoparticles

Condition A) A mixture of selected benzaldehyde (1.0 mmol) and phenylhydrazine (1.0 mmol) in the presence of 0.02 g MgO nanoparticles was reacted at 80°C. The reaction progress was monitored by thin-layer chromatography (TLC). After completion of the reaction, 10 ml of methanol was added to the mixture, and the solid catalyst was filtered through silica. The filtrate was placed in the ice bath to precipitate the product. Then the obtained crystals were separated through filter paper. The product was recrystallized in boiled ethanol to have purified crystals.

Condition B) to a 50 ml RBF, a solution of phenylhydrazine (1.0 mmol), selected benzaldehyde (1.0 mmol), and 15 ml of Methanol was added and the solution was irradiated in the presence of 0.05 g MgO nanoparticle for 90 minutes in a water bath of an ultrasonic cleaner at room temperature (to avoid increasing the vapor pressure of methanol, the power of the bath was adjusted on 50 KHz). The reaction progress was monitored by thin-layer chromatography (TLC). When the reaction was completed, the solid catalyst was filtered through silica and seperated from the reaction mixture. Then, the same procedure was performed to access pure products.

To obtain the following hydrazone derivatives the general procedure (A) was followed. The products were characterized by spectroscopic and physical techniques and the obtained data are aligned with previous reports [40–43].

Benzaldehyde phenylhydrazone (1a): Off-white solid (186mg, 95%). M.P_{rep} (°C) :152–154°C, IR(KBr)/ v(cm^{-1}): 3433.3 (NH), 3310 (C-H, aromatic), 1594.4 (N = C), 1489.01 (C = C, aromatic). ^{1}H NMR (400 MHz, DMSO-d_6) δ 10.33 (s, 1H), 7.85 (s, 1H), 7.67–7.60 (m, 4H), 7.36–7.34 (m, 2H), 7.30–7.25 (m, 1H), 7.20–7.16 (m, 2H), 7.09–7.01 (m, 2H), 6.74 (t, *J = 6.4* Hz, 1H).

(3-chloro-benzaldehyde) phenylhydrazone (2a): Off-white solid (223mg, 97%). M.P_{rep} (°C) :131–133°C, IR(KBr)/v(cm^{-1}): 3395.25 (NH), 3321.54 (C-H, aromatic), 1603.87 (N = C), 1457.98 (C-H, aromatic), 733.18 (C-Cl). ^{1}H NMR (400 MHz, DMSO-d_6) δ 10.52 (s, 1H, NH), 7.83 (s, 1H, N = CH), 7.70 (s, 1H, CH aromatic), 7.60 (d, *J = 7.6* Hz, 1H, CH aromatic), 7.40 (t, *J = 7.8* Hz, 1H, CH aromatic), 7.33 (d, *J = 7.7* Hz, 1H, CH aromatic), 7.21–7.25 (m, 2H, CH aromatic), 7.09 (d, *J = 7.9* Hz, 2H, CH aromatic), 6.77 (t, *J = 7.1* Hz, 1H, CH aromatic).

(4-chloro-benzaldehyde) phenylhydrazone (3a): Off-white solid (223mg, 97%). M.P_{rep} (°C) :120–122°C, IR(KBr)/v(cm^{-1}): 3429.25 (NH), 3311.10 (C-H, aromatic), 1598.87 (N = C), 1487.89 (C-H, aromatic), 749.02 (C-Cl). ^{1}H NMR (400 MHz, DMSO-d_6) δ 10.44 (s, 1H, NH), 7.84 (s, 1H, N = CH), 7.67 (d, *J = 8.3* Hz, 2H, CH aromatic), 7.44 (d, *J = 8.3* Hz, 2H, CH aromatic), 7.22 (t, *J = 7.7* Hz, 2H, CH aromatic), 7.07 (d, *J = 8.0* Hz, 2H, CH aromatic), 6.76 (t, *J = 7.2* Hz, 1H, CH aromatic).

(4-flouro-benzaldehyde) phenylhydrazone (4a): Off-white solid (199mg, 93%). M.P_{rep} (°C) :135–137°C, IR(KBr)/v(cm^{-1}): 3433.3 (NH), 3311.10 (C-H, aromatic), 1600.11 (N = C), 1260.44 (C-F). ^{1}H NMR (400 MHz, DMSO-d_6) δ 10.33 (s, 1H, NH), 7.86 (s, 1H, N = CH), 7.69 (dd, *J = 8.5, 5.4* Hz, 2H, CH aromatic), 7.29–7.13 (m, 4H, CH aromatic), 7.06 (d, *J = 8.0* Hz, 2H, CH aromatic), 6.75 (t, *J = 7.2* Hz, 1H, CH aromatic).

(2-nitro-benzaldehyde) phenylhydrazone (5a): Red solid (229mg, 95%). $M.P_{rep}$ (°C) :115–117°C, IR(KBr)/ v(cm^{-1}): 3462.97 (NH), 3296.71 (C-H, aromatic), 1600.74 (N = C), 1492.17, 1334.48 (N-O). ^{1}H NMR (400 MHz, DMSO-d_6) δ 10.89 (s, 1H, NH), 8.25 (s, 1H, N = CH), 8.16 (d, *J = 8.0* Hz, 1H, CH aromatic), 7.97 (d, *J = 8.1* Hz, 1H, CH aromatic), 7.71 (t, *J = 7.8* Hz, 1H, CH aromatic), 7.49 (t, *J = 7.7* Hz, 1H, CH aromatic), 7.24–7.28 (m, 2H, CH aromatic), 7.10 (d, *J = 7.9* Hz, 2H, CH aromatic), 6.82 (t, *J = 7.3* Hz, 1H, CH aromatic).

(3-nitro-benzaldehyde) phenylhydrazone (6a): Orange solid (229mg, 95%). $M.P_{rep}$ (°C) :117–119°C, IR(KBr)/v(cm^{-1}): 3410.59 (NH), 3321.99 (C-H, aromatic), 1589.56 (N = C), 1523.50, 1345.20 (N-O). ^{1}H NMR (400 MHz, DMSO-d_6) δ 10.69 (s, 1H), 8.43 (s, 1H), 8.08 (m, 2H), 7.95 (s, 1H), 7.65 (m, 1H), 7.29–7.15 (m, 2H), 7.11 (d, *J = 7.8* Hz, 2H), 6.78 (m, 1H).

(3-hydroxy-benzaldehyde) phenylhydrazone (7a): Off-white solid (191mg, 90%). $M.P_{rep}$ (°C) :143–145°C, IR(KBr)/v(cm^{-1}): 3520.79 (NH, OH), 3308.93 (C-H, aromatic), 1595.26 (N = C), 1255.23 (C-O). ^{1}H NMR (400 MHz, DMSO-d_6) δ 10.27 (s, 1H, NH), 9.43 (s, 1H, OH), 7.77 (s, 1H, N = CH), 7.15–7.23 (m, 3H, CH aromatic), 7.12–6.98 (m, 4H, CH aromatic), 6.68–6.74 (m, 2H, CH aromatic).

(4-hydroxy-benzaldehyde) phenylhydrazone (8a): Brown solid (193mg, 91%). $M.P_{rep}$ (°C) :169–171°C, IR(KBr)/v(cm^{-1}): 3427.51 (NH, OH), 3297.24 (C-H, aromatic), 1599.32 (N = C), 1255.42 (C-O). ^{1}H NMR (400 MHz, DMSO-d_6) δ 10.04 (s, 1H, NH), 9.63 (br, 1H, OH), 7.78 (s, 1H, N = CH), 7.47 (d, *J = 8.2* Hz, 2H, CH aromatic), 7.19 (t, *J = 7.7* Hz, 2H, CH aromatic), 7.01 (d, *J = 7.9* Hz, 2H, CH aromatic), 6.78 (d, *J = 8.2* Hz, 2H, CH aromatic), 6.70 (t, *J = 7.2* Hz, 1H, CH aromatic).

(2,4-dihydroxy-benzaldehyde) phenylhydrazone (9a): Off-white solid (189mg, 83%). $M.P_{rep}$ (°C) :165–167°C, IR(KBr)/v(cm^{-1}): 3378.21 (NH, OH), 3318.39 (C-H, aromatic), 1631.59 (N = C), 1601.20 (C-H) 1256.15 (C-O). ^{1}H NMR (400 MHz, DMSO-d_6) δ 10.74 (s, 1H, NH), 10.12 (s, 1H, OH), 9.67 (s, 1H, OH), 8.04 (s, 1H, N = CH), 7.28 (d, *J = 8.1* Hz, 1H, CH aromatic), 7.22 (t, *J = 7.7* Hz, 2H, CH aromatic), 6.90 (d, *J = 7.9* Hz, 2H, CH aromatic), 6.73 (s, 1H, CH aromatic), 6.32 (d, *J = 10.3* Hz, 2H, CH aromatic).

Benzophenone-N-phenylhydrazone (10a): Off-white solid (242mg, 89%). $M.P_{rep}$ (°C) :134–136°C, IR(KBr)/ v(cm^{-1}): 3321.87 (NH), 3051.88 (C-H, aromatic), 1594.24 (N = C), 1492.18 (C = C, aromatic). ^{1}H NMR (400 MHz, DMSO-d_6) δ 8.83 (s, 1H), 7.57 (m, 3H), 7.44 (m, 2H), 7.31 (m, 5H), 7.20 (m, 4H), 6.75 (m, 1H).

2-chloro-benzaldehyde (4-nitro-phenylhydrazone) (11a): Orange solid (264mg, 96%). $M.P_{rep}$ (°C) :245–247°C, IR(KBr)/v(cm^{-1}): 3433.20 (NH), 3270.36 (C-H, aromatic), 1592.18 (N = C), 1465.34, 1303.19 (N-O), 1105.23 (C-Cl). ^{1}H NMR (400 MHz, DMSO-d_6) δ 11.55 (s, 1H), 8.38 (s, 1H), 8.15 (d, *J = 8.9* Hz, 2H), 8.09–8.00 (m, 1H), 7.50 (dd, *J = 7.3*, 2.4 Hz, 1H), 7.43–7.35 (m, 2H), 7.19 (d, *J = 8.6* Hz, 2H). ^{13}C NMR (100 MHz, DMSO- d_6) δ 150.7, 139.4, 137.8, 132.7, 132.3, 131.0, 130.4, 128.0, 126.9, 126.6, 112.1.

3-chloro-benzaldehyde (4-nitro-phenylhydrazone) (12a): Orange solid (261mg, 95%). $M.P_{rep}$ (°C) :218–220°C, IR(KBr)/v(cm^{-1}): 3347.89 (NH), 3251.37 (C-H, aromatic), 1591.95 (N = C), 1474.85, 1300.30 (N-O),

1108.02 (C-Cl). ^{1}H NMR (400 MHz, DMSO-d_6) δ 11.42 (s, 1H), 8.13 (m, 2H), 8.01 (s, 1H), 7.80 (s, 1H), 7.68 (m, 1H), 7.42 (m, 2H), 7.19 (m, 2H). ^{13}C NMR (100 MHz, DMSO- d_6) δ 150.8, 140.4, 139.2, 137.5, 134.1, 131.1, 129.2, 126.6, 126.1, 125.6, 112.0.

4-fluoro-benzaldehyde (4-nitro-phenylhydrazone) (13a): Orange solid (246mg, 95%). M.P_{rep} (°C) :215–217°C, IR(KBr)/v(cm^{-1}): 3376.49 (NH), 3277.71 (C-H, aromatic), 1603.78 (N = C), 1495.73, 1316.15 (N-O), 1106.68 (C-F). ^{1}H NMR (400 MHz, DMSO-d_6) δ 11.30 (s, 1H, NH), 8.14 (d, *J = 8.9* Hz, 2H, CH aromatic), 8.05 (s, 1H, CH aromatic), 7.85–7.74 (m, 3H, CH aromatic), 7.28 (t, *J* = 8.5 Hz, 2H, CH aromatic), 7.23–7.11 (m, 2H, CH aromatic). ^{13}C NMR (100 MHz, DMSO-d_6) δ 163.1 (d, *J* = 246.8 Hz), 151.1, 141.2, 138.9, 131.8 (d, *J* = 3.0 Hz), 129 (d, *J* = 8.4 Hz), 126.6, 116.3 (d, *J* = 21.8 Hz), 111.7.

3-nitro-benzaldehyde (4-nitro-phenylhydrazone) (14a): Yellow solid (266mg, 93%). M.P_{rep} (°C) :257–259°C, IR(KBr)/v(cm^{-1}): 3433.23 (NH), 3269.49 (C-H, aromatic), 1588.81 (N = C), 1529.24, 1330.35 (N-O). ^{1}H NMR (400 MHz, DMSO-d_6) δ 11.54 (s, 1H), 8.53 (s, 1H), 8.22–8.00 (m, 5H), 7.76–7.63 (m, 1H), 7.28–7.16 (m, 2H). ^{13}C NMR (100 MHz, DMSO-d_6) δ 150.7, 148.8, 139.7, 139.5, 137.2, 132.8, 130.8, 126.6, 123.8, 121.0, 112.2.

3-hydroxy-benzaldehyde (4-nitro-phenylhydrazone) (15a): Yellow solid (231mg, 90%). M.P_{rep} (°C) :221–223°C, IR(KBr)/v(cm^{-1}): 3444.46 (NH, OH), 3256.89 (C-H, aromatic), 1592.54 (N = C), 1556.18, 1300.66 (N-O), 1109.00 (C-O). ^{1}H NMR (400 MHz, DMSO-d_6) δ 11.26 (s, 1H), 9.57 (s, 1H), 8.17–8.08 (m, 2H), 7.95 (s, 1H), 7.25–7.03 (m, 5H), 6.77 (d, *J* = 8.0 Hz, 1H). ^{13}C NMR (100 MHz, DMSO-d_6) δ 158.1, 151.1, 142.5, 138.8, 136.4, 130.3, 126.7, 118.5, 117.1, 112.8, 111.7.

4-methoxy-benzaldehyde (4-nitro-phenylhydrazone) (16a): Red solid (238mg, 88%). M.P_{rep} (°C) :165–167°C, IR(KBr)/v(cm^{-1}): 3447.56 (NH), 3266.78 (C-H, aromatic), 1608.45 (N = C), 1507.85, 1322.13 (N-O), 1108.07 (C-O). ^{1}H NMR (400 MHz, DMSO-d_6) δ 11.16 (s, 1H), 8.11 (d, *J* = 8.9 Hz, 2H), 7.99 (s, 1H), 7.67 (d, *J* = 8.3 Hz, 2H), 7.13 (d, *J* = 8.8 Hz, 2H), 6.99 (d, *J* = 8.4 Hz, 2H), 3.79 (s, 3H).

4-methyl-benzaldehyde (4-nitro-phenylhydrazone) (17a): Orange solid (237mg, 93%). M.P_{rep} (°C) :205–207°C, IR(KBr)/v(cm^{-1}): 3260.97 (NH), 3280.07 (C-H, aromatic), 1590.12 (N = C), 1542.74, 1302.71 (N-O). ^{1}H NMR (400 MHz, DMSO-d_6) δ 11.23 (s, 1H), 8.12 (d, *J* = 9.0 Hz, 2H), 8.01 (s, 1H), 7.62 (d, *J* = 7.8 Hz, 2H), 7.24 (d, *J* = 7.8 Hz, 2H), 7.15 (d, *J* = 8.9 Hz, 2H), 2.33 (s, 3H).

2,4-dimethoxy-benzaldehyde (4-nitro-phenylhydrazone) (18a): Orange solid (256mg, 85%). M.P_{rep} (°C) :189–191°C, IR(KBr)/v(cm^{-1}): 3303.47 (NH), 3245.07 (C-H, aromatic), 1603.17 (N = C), 1590.03, 1270.11 (N-O), 1180.24 (C-O). ^{1}H NMR (400 MHz, DMSO-d_6) δ 11.33 (s, 1H, NH), 8.35 (s, 1H, N = CH), 8.12 (d, *J* = 8.9 Hz, 2H, CH aromatic), 7.42 (d, *J* = 3.1 Hz, 1H, CH aromatic), 7.15 (d, *J* = 8.7 Hz, 2H, CH aromatic), 7.03 (d, *J* = 8.9 Hz, 1H, CH aromatic), 6.95 (dd, *J* = 9.1, 3.2 Hz, 1H, CH aromatic), 3.81 (s, 3H, OCH_3), 3.77 (s, 3H,

OCH_3). ^{13}C NMR (100 MHz, DMSO-d_6) δ 153.8, 152.1, 151.0, 138.8, 137.6, 126.6, 123.8, 116.8, 113.6, 111.7, 109.7, 56.7, 55.9.

2,4-dihydroxy-benzaldehyde (4-nitro-phenylhydrazone) (19a): Red solid (237mg, 87%). $M.P_{rep}$ (°C) :191–193°C, IR(KBr)/v(cm^{-1}): 3258.72(NH, OH), 3092.69(C-H, aromatic), 1593.57 (N = C), 1493.42, 1320.45 (N-O). ^1H NMR (400 MHz, DMSO-d_6) δ 11.10 (s, 1H), 10.16 (s, 1H), 9.78 (s, 1H), 8.23 (s, 1H), 8.10 (d, *J* = 8.9 Hz, 2H), 7.50 (d, *J* = 9.1 Hz, 1H), 7.01 (d, *J* = 8.9 Hz, 2H), 6.32 (dt, *J* = 4.9, 2.5 Hz, 2H).

Acetone-(4-nitro-phenylhydrazone) (20a): Yellow solid (162mg, 84%). $M.P_{rep}$ (°C) :145–147°C, IR(KBr)/ v(cm^{-1}): 3428.18 (NH), 3322.01 (C-H, aromatic), 1603.44 (N = C), 1473.17, 1306.99 (N-O). ^1H NMR (400 MHz, DMSO-d_6) δ 9.77 (s, 1H), 8.08 (d, *J* = 9.0 Hz, 2H), 7.15 (d, *J* = 8.9 Hz, 2H), 2.01 (s, 3H), 1.96 (s, 3H). ^{13}C NMR (100 MHz, DMSO-d_6) δ 152.2, 150.0, 138.1, 126.4, 111.6, 25.6, 17.6.

Acetophenone-(4-nitro-phenylhydrazone) (21a): Orange solid (222mg, 87%). $M.P_{rep}$ (°C): 185–187°C, IR(KBr)/v(cm^{-1}): 3311.09 (NH), 1595.97 (N = C), 1469.99, 1317.25 (N-O). ^1H NMR (400 MHz, DMSO-d_6) δ 10.23 (s, 1H), 8.16 (d, *J* = 8.8 Hz, 2H), 7.86 (d, *J* = 7.7 Hz, 2H), 7.44 (m, 2H), 7.37 (m, 3H), 2.36 (s, 3H). ^{13}C NMR (100 MHz, DMSO-d_6) δ 151.9, 146.6, 139.0, 138.9, 129.1, 128.9, 126.4, 126.3, 112.5, 14.0.

Benzophenone-(4-nitro-phenylhydrazone) (22a): Yellow solid (266mg, 84%). $M.P_{rep}$ (°C):151–153°C, IR(KBr)/v(cm^{-1}): 3316.31 (NH), 1596,16(N = C), 1501,77, 1318,15 (N-O). ^1H NMR (400 MHz, DMSO-d_6) δ 9.90 (s, 1H), 8.12 (d, *J* = 9.0 Hz, 2H), 7.62 (d, *J* = 7.8 Hz, 2H), 7.52–7.47 (m, 3H), 7.43–7.34 (m, 7H).

2-nitro-benzaldehyde (4-bromo-phenylhydrazone) (23a): Purple solid (287mg, 90%). $M.P_{rep}$ (°C) :167–169°C, IR(KBr)/v(cm^{-1}): 3393.87 (NH), 3293.02 (C-H, aromatic), 1535.27 (N = C), 1484.19, 1254.55 (N-O). ^1H NMR (400 MHz, DMSO-d_6) δ 11.00 (s, 1H), 8.27 (s, 1H), 8.16 (d, *J* = 7.9 Hz, 1H), 7.98 (d, *J* = 8.2 Hz, 1H), 7.78–7.66 (m, 1H), 7.52 (s, 1H), 7.41 (d, *J* = 8.5 Hz, 2H), 7.06 (d, *J* = 8.4 Hz, 2H).

3-nitro-benzaldehyde (4-bromo-phenylhydrazone) (24a): Yellow solid (293mg, 92%). $M.P_{rep}$ (°C) :147–149°C, IR(KBr)/v(cm^{-1}): 3414.12 (NH), 3322.51 (C-H, aromatic), 1584.66 (N = C), 1479.26, 1262.31 (N-O). ^1H NMR (400 MHz, DMSO-d_6) δ 10.81 (s, 1H, NH), 8.45 (s, 1H, N = CH), 8.10–8.12 (m, 2H, CH aromatic), 7.98 (s, 1H, CH aromatic), 7.67 (t, J = 7.9 Hz, 1H, CH aromatic), 7.41 (d, *J* = 8.6 Hz, 2H, CH aromatic), 7.08 (d, *J* = 8.5 Hz, 2H, CH aromatic).

3-hydroxy-benzaldehyde (4-bromo-phenylhydrazone) (25a): Off-white solid (258mg, 89%). $M.P_{rep}$ (°C) :163–169°C, IR(KBr)/v(cm^{-1}): 3381.73 (NH, OH), 3307.42 (C-H, aromatic), 1588.51 (N = C), 1249.89 (C-O).^1H NMR (400 MHz, DMSO-d_6) δ 10.40 (s, 1H, NH), 9.44 (s, 1H, OH), 7.79 (s, 1H, N = CH), 7.37 (d, *J* = 8.5 Hz, 2H, CH aromatic), 7.18 (t, *J* = 7.9 Hz, 1H, CH aromatic), 7.10 (s, 1H, CH aromatic), 7.01 (dd, *J* = 13.0, 8.2 Hz, 3H, CH aromatic), 6.71 (d, *J* = 7.6 Hz, 1H, CH aromatic). ^{13}C NMR (100 MHz, DMSO-d_6) δ 158.0, 145.1, 138.1, 137.3, 132.2, 130.1, 117.8, 116.1, 114.3, 112.2, 109.9.

Benzophenone-(4-bromo-phenylhydrazone) (26a): Off-white solid (332mg, 95%). $M.P_{rep}$ (°C) :103–105°C, IR(KBr)/v(cm^{-1}): 3403.38 (NH), 3324.26 (C-H, aromatic), 1590.72 (N = C). ^{1}H NMR (400 MHz, DMSO-d_6) δ 9.03 (s, 1H), 7.62–7.55 (m, 3H), 7.48–7.42 (m, 2H), 7.36–7.30 (m, 7H), 7.25–7.19 (m, 2H).

Acetophenone-(2,4-dinitro-phenylhydrazone) (27a): Orange solid (279mg, 93%). $M.P_{rep}$ (°C) :241–243°C, IR(KBr)/v(cm^{-1}): 3360.43 (NH), 3302.51 (C-H, aromatic), 1612.07 (N = C), 1504.42, 1324.12 (N-O). ^{1}H NMR (400 MHz, DMSO-d_6) δ 11.12 (s, 1H), 8.92 (s, 1H), 8.44 (d, *J* = 9.8 Hz, 1H), 8.12 (d, *J* = 9.9 Hz, 1H), 7.99–7.93 (m, 2H), 7.52–7.46 (m, 3H), 2.49 (s, 3H).

3-methyl-acetophenone (2,4-dinitro-phenylhydrazone) (28a): Orange solid (289mg, 92%). $M.P_{rep}$ (°C) :199–201°C, IR(KBr)/v(cm^{-1}): 3360.43 (NH), 3302.51 (C-H, aromatic), 1612.07 (N = C), 1504.42, 1324.12 (N-O). ^{1}H NMR (400 MHz, DMSO-d_6) δ 11.11 (s, 1H), 8.91 (s, 1H), 8.44 (d, *J* = 9.7 Hz, 1H), 8.11 (d, *J* = 9.6 Hz, 1H), 7.75 (d, *J* = 9.4 Hz, 2H), 7.42–7.35 (m, 1H), 7.31 (s, 1H), 2.47 (s, 3H), 2.41 (s, 3H). ^{13}C NMR (100 MHz, DMSO-d_6) δ 153.9, 145.0, 138.3, 137.8, 137.6, 131.1, 130.7, 130.3, 129.0, 127.5, 124.2, 123.5, 117.0, 21.6, 14.0.

4. RESULTS and DISCUSSIONS

The structure of the synthesized magnesium oxide nanoparticle was confirmed by various analysis, including X-ray diffractometer (XRD), transmission electron microscope (TEM), and scanning electron microscope (SEM).

4.1. Characterization of the MgO nanocrystals

The XRD pattern of the synthesized MgO sample is demonstrated in Fig. 2. All the peaks matches the standard values of JCPDS 45–946 and could be indexed to cubic MgO crystallites with the lattice parameter a = 0.421 nm. In Fig. 2, no extra peaks were observed which means the high purity of synthesized nanoparticles.

The related XRD pattern of the synthesized MgO nanoparticles represented two main broad peaks. The diffraction peaks at 2θ values of 37°, 42°, 62°, 74°, and 78° correspond to (1 1 1), (2 0 0), (3 1 1), and (2 2 2) diffraction planes of cubic MgO, respectively. To calculate the average crystallite sizes of the magnesium oxide, we used the Debye–Scherrer's equation; D = 0.9l/bCosθ. In this equation, D is represented the crystallite size, b is the full width at half maximum (FWHM) in radians of the diffraction peaks, θ is the Bragg's diffraction angle, and l is the X-ray wavelength (1.54056 A°). Based on the FWHM of the most intense plane (2 0 0), the crystallite size is calculated and the results showed that the size of the synthesized MgO nanoparticles most be around 16 nm. The pattern of the MgO nanoparticles indicated the cubic phase which has high similarity to the reported values (JCPDS No. 45–946).

The scanning electron microscop (SEM) images of the MgO nanoparticles is represented in Fig. 3. As it is illustrated, the obtained SEM images of synthesized MgO nanoparticles is confirmed the nano size of the

compound and the size of nanoparticles is found between 30–50 nm.

To study the quantitative compositional information in synthesized MgO nanoparticle and reveal its elemental identification, the Energy Dispersive X-Ray Analyzer (EDX or EDA) was also operated (Fig. 4). The EDX analysis is applied to detect present elements on nanoscale areas. The elemental detection proved the presence of Mg and O elements in the desired ratio expected in MgO.

4.2. Catalytic studies

Herein, a one-pot condensation reaction of aryl hydrazines and substituted benzaldehydes or ketones catalyzed by MgO nanoparticles is reported under solvent-free and ultrasonic conditions. In the present synthetic method, the Aryl hydrazones were achieved with high outcome and satisfying times. In follow, the optimization procedures have been investigated for both conditions and the results will be compared.

Optimization conditions for procedure A) to initiate the study, the reaction between phenylhydrazine and benzaldehyde was chosen as a standard condition. Firstly, the reaction was performed without using catalyst and solvent at 80°C and poor results were obtained (Table 1, entry 1). Next, the reaction was carried out using various amounts of the catalyst under solvent-free conditions at 80°C (Table 1, entry 2–6). When 0.01 g of MgO nanoparticle was applied, the yield raised to 31% in 40 minutes. Subsequently, increasing the amount of the catalyst improved the outcome. It was found that loading 0.03 g of the catalyst has the highest efficiency and lead to complete the reaction after 30 min (Table 1, entry 5). Increasing the applied amount of the catalyst led to no improvements (Table 1, entry 6). The effect of temperature on the reaction performance was also studied (Table 2). Running the reaction at ambient temperature using 0.03 g of the catalyst for 120 minutes resulted in 23% (Table 2, entry 1). By increasing the temperature the yield of the reaction was enhanced and the reaction completed in shorter time (Table 2, entries 2–6). Consequently, the reaction temperature was optimized at 80°C in 30 minutes to have the highest productivity of the reaction (Table 2, entry 5).

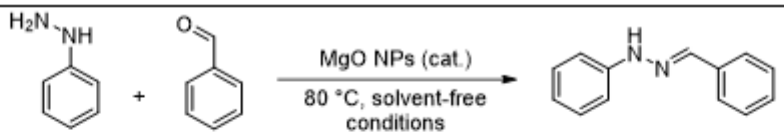

Entry	MgO NPs (g)	Time (min)	Yield (%)
1	-	40	<10
2	0.01	40	31
3	0.02	40	62
4	0.01	35	85
5	0.03	30	95
6	0.05	30	95

Reaction conditions: phenylhydrazine 1.0 mmol, and benzaldehyde 1.0 mmol

Table 2
Effect of temperature on the hydrazone formation

Entry	Temperature (°C)	Time (min)	Yield (%)
1	rt	120	23
2	50	60	36
3	60	30	55
4	70	30	87
5	80	30	95
6	100	30	95
Reaction conditions: phenylhydrazine 1.0 mmol, benzaldehyde 1.0 mmol, and MgO NPs 0.03 g as the catalyst			

Optimization conditions for procedure B): to continue our investigations on the reaction conditions, the reaction between phenylhydrazine and benzaldehyde was studied under ultrasonic conditions as well. To start the optimizing studies, we performed the reaction in the prescence of 0.02 g of MgO nanoparticles in 50 kHz ultrasonic bath at ambient temperature for 120 minutes (Table 3, entry 1) and resulted in 38% yield of the desired product. Increasing the amount of loaded catalyst resulted in increasing the outcome (Table 3, entries 2–4) and the reaction had the highest efficiency in the presence of 0.06 g MgO nanoparticles. Moreover, the reaction was performed in 90 and 60 minutes (Table 3, entries 5 and 6). It was found that the reaction needs at least 90 minutes to complete. In order to reveal the effect of the catalyst on the yield of the reaction, no catalyst was and, the poor results were achieved (Table 3, entry 7). Furthermore, the effect of solvent on the reaction performance was investigated. Hence, the reaction was carried out in various solvents and, Methanol was chosen as the best solvent for the desired transformation (Table 4, entries 1–5). Finally, the yield of the reaction was sharply dropped to 19% under neat conditions (Table 4, entry 6).

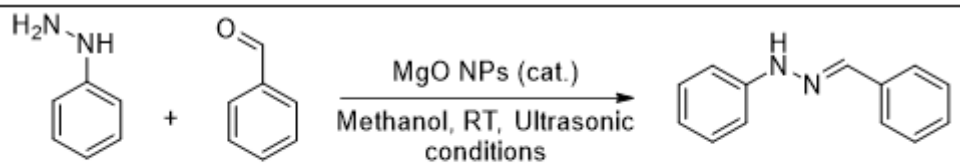

Entry	MgO NPs (g)	Time (min)	Yield (%)
1	0.02	120	38
2	0.04	120	67
3	0.05	120	83
4	0.06	120	91
5	**0.06**	**90**	**91**
6	0.06	60	84
7	-	90	<5

Reaction conditions: phenylhydrazine 1.0 mmol, benzaldehyde 1.0 mmol, in 15 ml methanol under ultrasonic irradiation.

Table 4
Effect of solvent on the hydrazone formation

Entry	Solvents (°C)	Yield (%)
1	Ethanol	82
2	**Methanol**	**91**
3	Ethyl acetate	79
4	Dichloromethane	73
5	Acetone	89
6	neat	19

Reaction conditions: phenylhydrazine 1.0 mmol, benzaldehyde 1.0 mmol, Solvent 15 ml, and MgO NPs 0.06 g as the catalyst

Based on the obtained results, the reaction has a better outcome under solvent-free conditions. On the other side, the neat condition has priority to using solvents, although the temperature factor is lower in procedure B in comparison to procedure A. According to this, we select the solvent-free pathway as the standard condition and, the scope of the reaction is explored under the solvent-free protocol. The novelty of presented protocol is employing of MgO nanoparticles as a green nanocatalyst and economical process owing to the usage of equimolar amounts of starting materials. Because of the special features of MgO nanoparticles, including their stability and eco-friendly merits, they have attracted much interest in synthetic methods. Additionally, the synthesis of hydrazones under solvent-free conditions is a notable merit.

The efficiency of MgO nanoparticles is owing to the activity of the catalyst surface, which is promoted the condensation reaction in a short time. To investigate the reaction conditions more deeply, the effect of

various functional groups on the reaction efficiency was studied. The reaction was carried out in the presence of several substituents on the aryl hydrazines and benzaldehydes. The results are outlined in Table 5. The scope investigation of the reaction revealed that various aromatic benzaldehydes, ketones, and aryl hydrazines bearing electron-withdrawing and electron-donating groups led to corresponding hydrazones with high yields. Moreover, the reaction worked well with aliphatic ketones like acetone (Table 5).

The mechanism of the reaction could be explained by the dual effect of MgO nanoparticles in the reaction. Since the MgO nanoparticles possess acid-base bifunctional sites in their structure, the presented Mg and O elements can behave as weak Lewis acidic sites and Brönsted basic sites with high strength activity, respectively [30]. The lewis acid cites of MgO NPs can coordinate the aldehyde or ketone functional groups and activate them for nucleophilic attack. On the other side, the basic sites of MgO NPs facilitate the removal of water and the formation of an imine double bond to achieve the final products.

CONCLUSION

In this protocol, a promising and green procedure to access aryl hydrazones through condensation reaction between equimolar amounts of Aryl hydrazines and aromatic aldehydes and ketones catalyzed by MgO NPs is presented. This novel method has significant advantages, including high product yields, solvent-free conditions, no side products, short reaction time, and an easy product purification process.

Declarations

Ethical Approval

This declaration is “not applicable”.

Competing interests

The authors have no conflicts of interest to declare that are relevant to the content of this article.

Authors' contributions

All of the authors contributed to the design and implementation of the research, to the analysis of the results, and to the writing of the manuscript.

Funding

This work was supported by the “University of Kashan”.

Availability of data and materials

The data that support the findings of this study are openly available within the article and its supplementary material file.

References

1. a) de Oliveira Carneiro Brum, Juliana; França, T. C. C.; LaPlante, S. R.; Villar, J. D. F. *MRMC* **2020**, *20*, 342–368; b) Kölmel, D. K.; Kool, E. T. *Chem. Rev.* **2017**, *117*, 10358–10376; c) Shao, B.; Qian, H.; Li, Q.; Aprahamian, I. *J. Am. Chem. Soc.* **2019**, *141*, 8364–8371; d) Sharma, P. C.; Sharma, D.; Sharma, A.; Saini, N.; Goyal, R.; Ola, M.; Chawla, R.; Thakur, V. K. *Materials Today Chemistry* **2020**, *18*, 100349; e) Wang, G.; Zhang, Q.; Zhu, F.; Zhang, C.; Li, H.; Lu, J. *J. Mater. Chem. C* **2021**, *9*, 6351–6356;
2. Alam, M.; Verma, G.; Shaquiquzzaman, M.; Marella, A.; Akhtar, M.; Ali, M. *J Pharm Bioall Sci* **2014**, *6*, 69.
3. a) El-Etrawy, A.-A. S.; Sherbiny, F. F. *Journal of Molecular Structure* **2021**, *1232*, 129993; b) Matson, J. B.; Stupp, S. I. *Chem. Commun.* **2011**, *47*, 7962; c) Ollivier, N.; Agouridas, V.; Snella, B.; Desmet, R.; Drobecq, H.; Vicogne, J.; Melnyk, O. *Org. Lett.* **2020**, *22*, 8608–8612; d) Richardson, B. M.; Walker, C. J.; Maples, M. M.; Randolph, M. A.; Bryant, S. J.; Anseth, K. S. *Adv. Healthcare Mater.* **2021**, *10*, 2002030; e) Sharma, P. K.; Singh, Y. *Biomacromolecules* **2019**, *20*, 2174–2184;
4. Prieto, A.; Bouyssi, D.; Monteiro, N. *Eur. J. Org. Chem.* **2018**, *2018*, 2378–2393.
5. a) Akbari Afkhami, F.; Mahmoudi, G.; Miroslaw, B.; Qu, F.; Gupta, A.; Frontera, A.; Zubkov, F. I.; Zangrando, E.; Safin, D. A. *New J. Chem.* **2020**, *44*, 9429–9437; b) Ayyannan, G.; Mohanraj, M.; Gopiraman, M.; Uthayamalar, R.; Raja, G.; Bhuvanesh, N.; Nandhakumar, R.; Jayabalakrishnan, C. *Inorganica Chimica Acta* **2020**, *512*, 119868; c) Babahan, I.; Özmen, A.; Aksel, M.; Bilgin, M. D.; Gumusada, R.; Gunay, M. E.; Eyduran, F. *Appl Organomet Chem* **2020**, *34*, 377; d) Sıdır, İ.; Sıdır, Y. G.; Berber, H.; Demiray, F. *Journal of Molecular Structure* **2019**, *1176*, 31–46;
6. Aysha, T.; Zain, M.; Arief, M.; Youssef, Y. *Heliyon* **2019**, *5*, e02358.
7. a) Lygaitis, R.; Getautis, V.; Grazulevicius, J. V. *Chem. Soc. Rev.* **2008**, *37*, 770; b) Petrus, M. L.; Sirtl, M. T.; Closs, A. C.; Bein, T.; Docampo, P. *Mol. Syst. Des. Eng.* **2018**, *3*, 734–740; c) Yin, X.; Song, Z.; Li, Z.; Tang, W. *Energy Environ. Sci.* **2020**, *13*, 4057–4086;
8. a) Kajal, A.; Bala, S.; Sharma, N.; Kamboj, S.; Saini, V. *International Journal of Medicinal Chemistry* **2014**, *2014*, 1–11; b) Qi, P.; Wu, X.; Liu, L.; Yu, H.; Song, S. *Front. Pharmacol.* **2018**, *9*, 1337; c) Wahbeh, J.; Milkowski, S. *SLAS TECHNOLOGY: Translating Life Sciences Innovation* **2019**, *24*, 161–168;
9. a) Aprahamian, I. *Chem. Commun.* **2017**, *53*, 6674–6684; b) Gurbanov, A. V.; Kuznetsov, M. L.; Demukhamedova, S. D.; Alieva, I. N.; Godjaev, N. M.; Zubkov, F. I.; Mahmudov, K. T.; Pombeiro, A. J. L. *CrystEngComm* **2020**, *22*, 628–633; c) Su, X.; Aprahamian, I. *Chem. Soc. Rev.* **2014**, *43*, 1963; d) Villada, J. D.; D'Vries, R. F.; Macías, M.; Zuluaga, F.; Chaur, M. N. *New J. Chem.* **2018**, *42*, 18050–18058;
10. a) Canal-Martín, A.; Pérez-Fernández, R. *ACS Omega* **2020**, *5*, 26307–26315; b) Hewitt, S. H.; Wilson, A. J. *Eur. J. Org. Chem.* **2018**, *2018*, 1872–1879; c) Higgs, P. L.; Ruiz-Sanchez, A. J.; Dalmina, M.; Horrocks, B. R.; Leach, A. G.; Fulton, D. A. *Org. Biomol. Chem.* **2019**, *17*, 3218–3224;

11. a) Ghosh, B.; Balhara, R.; Jindal, G.; Mukherjee, S. *Angew. Chem. Int. Ed.* **2021**, *60*, 9086–9092; b) Heravi, M. M.; Rohani, S.; Zadsirjan, V.; Zahedi, N. *RSC Adv.* **2017**, *7*, 52852–52887; c) Hughes-Whiffing, C. A.; Perry, A. *Org. Biomol. Chem.* **2021**, *19*, 627–634;
12. Lazny, R.; Nodzewska, A. *Chem. Rev.* **2010**, *110*, 1386–1434.
13. a) Panda, N.; Ojha, S. *Journal of Organometallic Chemistry* **2018**, *861*, 244–251; b) Senöz, H.; Yildirim, E.; Tezcan, H. *Asian J. Chem.* **2013**, *25*, 2989–2993;
14. a) Fernandes, M.; RB Singh, K.; Sarkar, T.; Singh, P.; Pratap Singh, R. *Adv. Mater. Lett.* **2020**, *11*, 1–10; b) Yaqoob, A. A.; Ahmad, H.; Parveen, T.; Ahmad, A.; Oves, M.; Ismail, I. M. I.; Qari, H. A.; Umar, K.; Mohamad Ibrahim, M. N. *Front. Chem.* **2020**, *8*, 11;
15. Jeevanandam, J.; Chan, Y. S.; Danquah, M. K. *ChemistrySelect* **2017**, *2*, 10393–10404.
16. Thamban Chandrika, N.; Dennis, E. K.; Brubaker, K. R.; Kwiatkowski, S.; Watt, D. S.; Garneau-Tsodikova, S. *ChemMedChem* **2021**, *16*, 124–133.
17. Lynch, B. M.; Pausacker, K. H. *J. Chem. Soc.* **1954**, 1131.
18. Creencia, E. C.; Kosaka, M.; Muramatsu, T.; Kobayashi, M.; Iizuka, T.; Horaguchi, T. *J. Heterocyclic Chem.* **2009**, *46*, 1309–1317.
19. Dadiboyena, S.; Valente, E. J.; Hamme, A. T. *Tetrahedron Letters* **2009**, *50*, 291–294.
20. Al-Sehemi, A. G.; Irfan, A.; Al-Melfi, M. A. M.; Al-Ghamdi, A. A.; Shalaan, E. *Journal of Photochemistry and Photobiology A: Chemistry* **2014**, *292*, 1–9.
21. Dutta Gupta, S.; Revathi, B.; Mazaira, G. I.; Galigniana, M. D.; Subrahmanyam, C.; Gowrishankar, N. L.; Raghavendra, N. M. *Bioorganic Chemistry* **2015**, *59*, 97–105.
22. Ye, J.; Bellotti, P.; Paulisch, T. O.; Daniliuc, C. G.; Glorius, F. *Angew. Chem. Int. Ed.* **2021**, *60*, 13671–13676.
23. Turkoglu, G.; Berber, H.; Kani, I. *New J. Chem.* **2015**, *39*, 2728–2740.
24. Buzykin, B. I.; Titova, Z. S.; Cherepinskii-Malov, V. D.; Gazetdinova, N. G.; Stolyarov, A. P.; Litvinov, I. A.; Struchkov, Y. T.; Kitaev, Y. P. *Russ Chem Bull* **1983**, *32*, 485–491.
25. Barton, D. H.; Okano, T.; Parekh, S. I. *Tetrahedron* **1991**, *47*, 1823–1836.
26. Maharramov, A. M.; Shikhaliyev, N. Q.; Suleymanova, G. T.; Gurbanov, A. V.; Babayeva, G. V.; Mammadova, G. Z.; Zubkov, F. I.; Nenajdenko, V. G.; Mahmudov, K. T.; Pombeiro, A. J. *Dyes and Pigments* **2018**, *159*, 135–141.
27. Shikhaliyev, N. G.; Maharramov, A. M.; Suleymanova, G. T.; Babayeva, G. V.; Mammadova, G. Z.; Shikhaliyeva, I. M.; Babazade, A. A.; Nenajdenko, V. G.; Joule, J. A. *Arkivoc* **2021**, *2021*, 67–75.
28. Köhling, P.; Schmidt, A. M.; Eilbracht, P. *Org. Lett.* **2003**, *5*, 3213–3216.
29. Yoshimura, A.; Banek, C. T.; Yusubov, M. S.; Nemykin, V. N.; Zhdankin, V. V. *J. Org. Chem.* **2011**, *76*, 3812–3819.
30. MIRZAEI, H.; DAVOODNIA, A. *Chinese Journal of Catalysis* **2012**, *33*, 1502–1507.

Table 5

Table 5 is available in the Supplementary Files section.

Figures

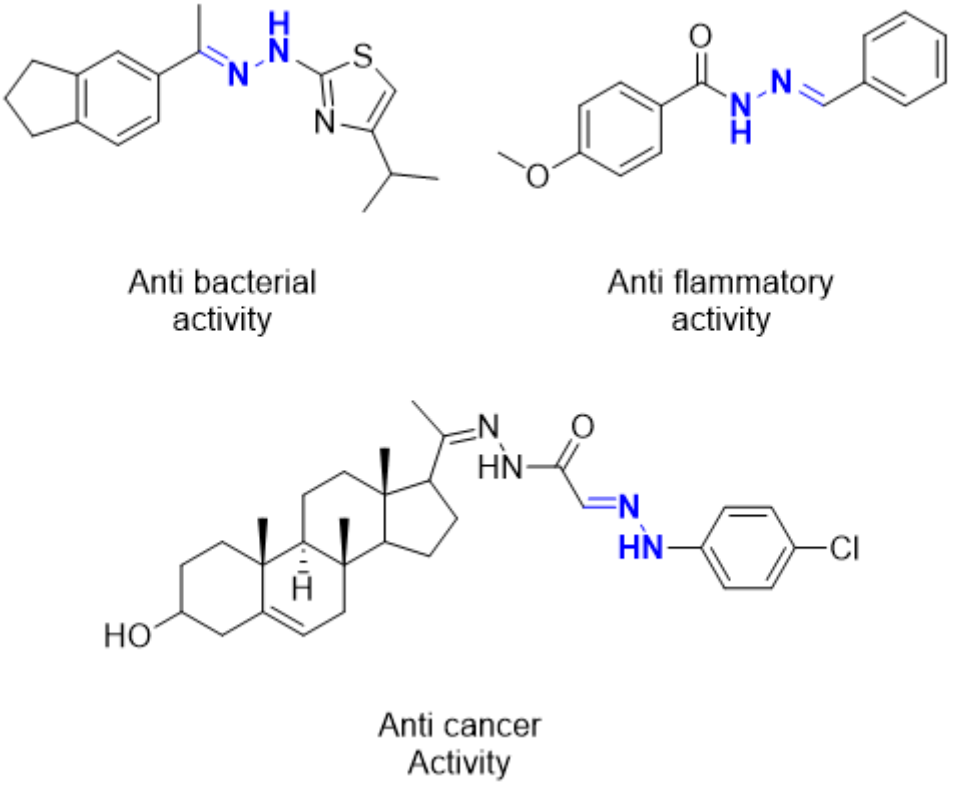

Figure 1

Hydrazone-containing structures with biological activities

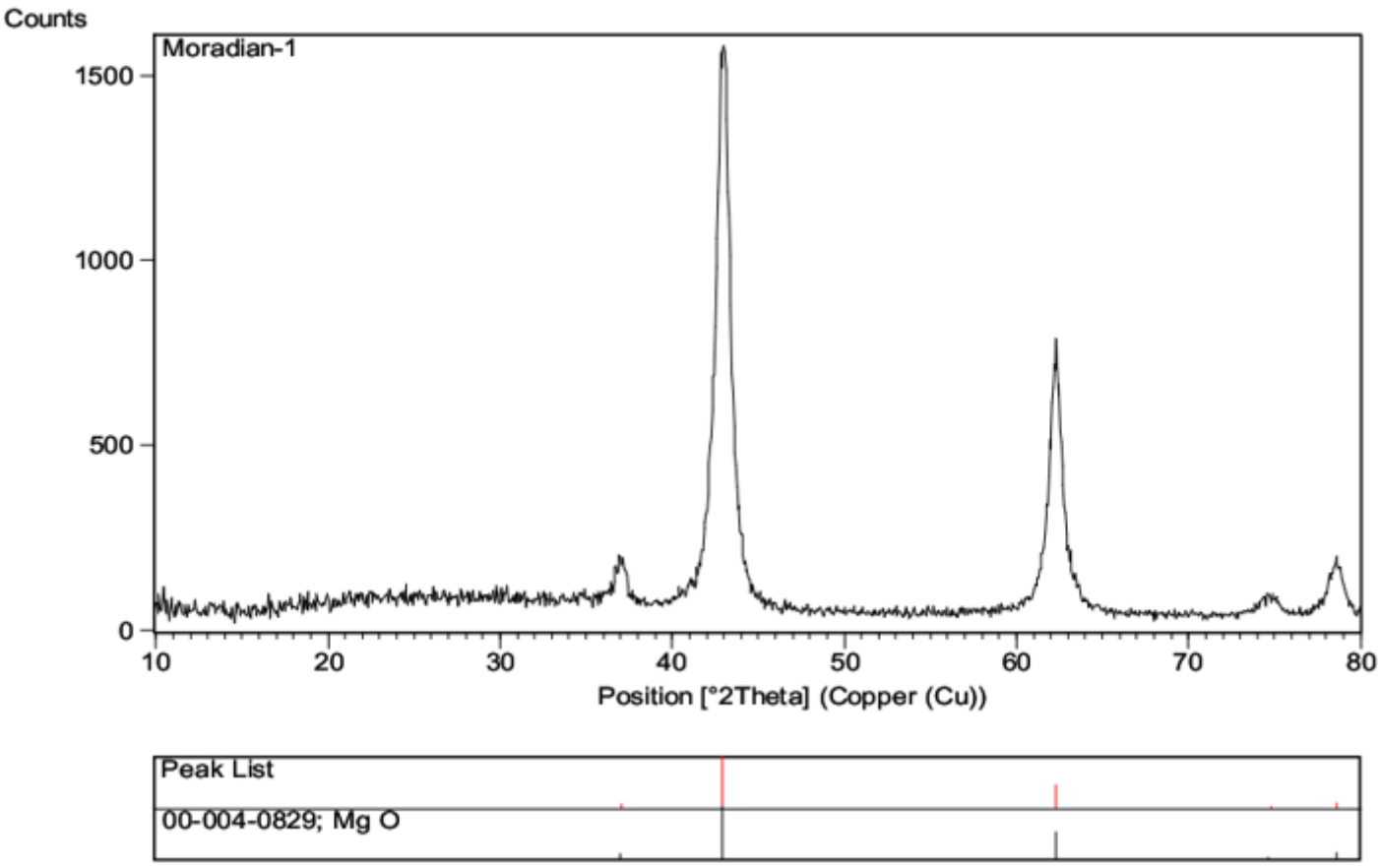

Figure 2

The XRD pattern of MgO nanoparticles

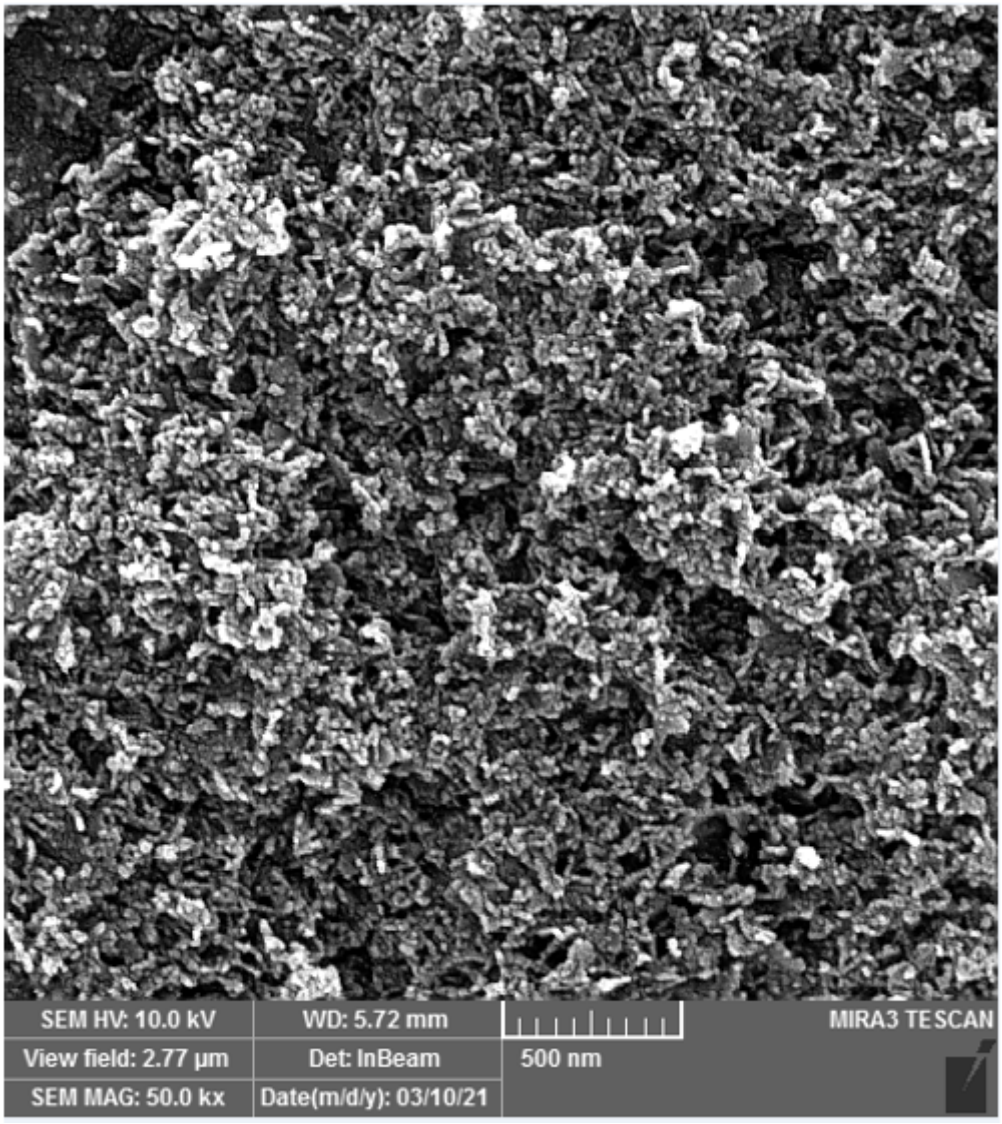

Figure 3

SEM images of synthesized MgO nanoparticles

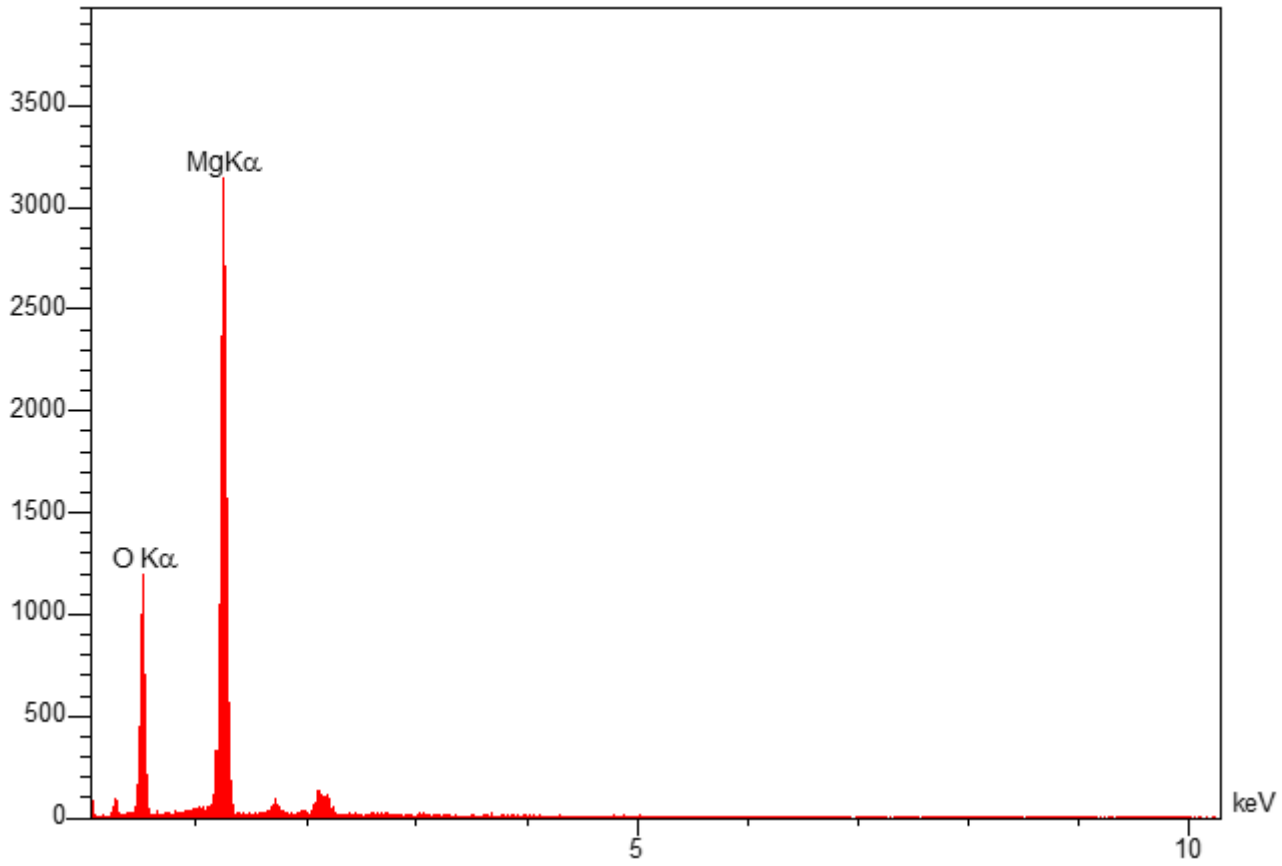

Figure 4

Energy dispersive X-ray (EDX) spectra of MgO nanoparticles

Supplementary Files

This is a list of supplementary files associated with this preprint. Click to download.

- MoradiCSSI.pdf
- table5.docx